



Molecular dynamics calculation of carbon/hydrocarbon reflection coefficients on a hydrogenated graphite surface

D.A. Alman ^{*}, D.N. Ruzic

University of Illinois, 214 Nuclear Engineering Laboratory, 103 S. Goodwin Avenue, Urbana, IL 61801, USA

Abstract

Reflection coefficients for carbon atoms and hydrocarbon molecules on a carbon surface are critically needed for plasma–surface interaction analysis of carbon surfaces. These coefficients have been calculated with a molecular dynamics code using the Brenner hydrocarbon potential. The surface was prepared by bombarding a pure graphite lattice with energetic hydrogen, until a saturation was reached at ~ 0.42 H:C. Carbon atoms and several hydrocarbons (CH, CH₂, CH₃, and CH₄) were incident on this surface at different energies and angles. Typical results for carbon incident at 45° show reflection coefficients of 0.64 ± 0.01 at thermal energy, decreasing to 0.19 ± 0.01 at 10 eV. Hydrocarbons show more complicated behavior, tending to reflect as molecules at thermal energies and break up at higher energies, producing a spectrum of different reflected species. The total reflection of carbon via these fragments tends to decrease with incident energy, and increase with hydrogen content in the original molecule. The reflection coefficients, together with the energy and angular distribution of reflected particles, can be incorporated in erosion/redeposition codes to allow improved modeling of chemically eroded carbon transport in fusion devices.

© 2003 Elsevier Science B.V. All rights reserved.

PACS: 54.40.Hf; 81.05.Uw

Keywords: Reflection; Carbon; Hydrocarbon; Molecular dynamics; Plasma facing components; Erosion/redeposition

1. Introduction

The choice of wall materials in fusion devices is critical to overall performance. Carbon based materials, including graphite and carbon fiber composites, are frequently chosen as a plasma facing component (PFC) material. Carbon has the advantages of a low atomic number and excellent thermal properties necessary to withstand the required heat loads. However, carbon is susceptible to chemical sputtering when bombarded by hydrogen from the plasma. The result is the release of various hydrocarbon impurities into the plasma. These

are generally dominated by methane, but heavier hydrocarbons (C₂H_y and C₃H_y species) can account for a majority of the total chemical erosion at low incident energies [1].

Computer modeling is widely used to study the performance of PFC materials. Erosion/redeposition codes, WBC [2] for example, can investigate key issues such as: (1) net erosion rates and wall lifetime, (2) tritium codeposition, and (3) core plasma contamination. The procedure is to launch impurities from the wall, and track them through the boundary plasma until they leave the near surface region or strike a surface. Particles that return to a surface are generally considered to be redeposited. A critical improvement to such a method is to include realistic reflection/sticking coefficients, so that impurities returning to the wall can either stick (and count as being redeposited) or continue back into the

^{*} Corresponding author. Tel.: +1-217 333 1750; fax: +1-217 333 2906.

E-mail address: alman@uiuc.edu (D.A. Alman).

edge plasma, as appropriate. Modeling of carbon based PFCs requires this information for all hydrocarbon molecules that come about from chemical sputtering.

2. Computational method

A molecular dynamics (MD) code, MolDyn [3], was modified to study reflection of carbon and hydrocarbon molecules on a hydrogenated carbon (C:H) film. The code uses parameter set II of the Brenner hydrocarbon potential [4], an empirical many-body potential based on the Abell– Tersoff covalent bonding formalism [5,6]. This potential describes reasonably well the chemical bonding in graphite and diamond lattices, as well as hydrocarbon molecules. The second parameter set was chosen because it gives more accurate C–C bond stretching force constants. Temperature is controlled in the simulations with the velocity scaling method of Berendsen [7]. The simulation cell begins as a pure graphite {0–10} lattice that is 39.1 Å by 40.2 Å and 20.1 Å deep, containing 4032 carbon atoms, and is modified as described below. Boundary conditions were chosen to simulate a small region of a much larger bulk material. The atoms within 2 Å of the bottom surface are held fixed, the top surface is free, and the sides of the cell have periodic boundary conditions.

2.1. Surface preparation

In order to study a surface more relevant to fusion devices, the original surface was held at 300 K and bombarded with hydrogen atoms at 20 eV and 45° (roughly what might occur in a tokamak) until the surface was saturated with hydrogen. The evolution of the lattice, in terms of hydrogen content, is shown in

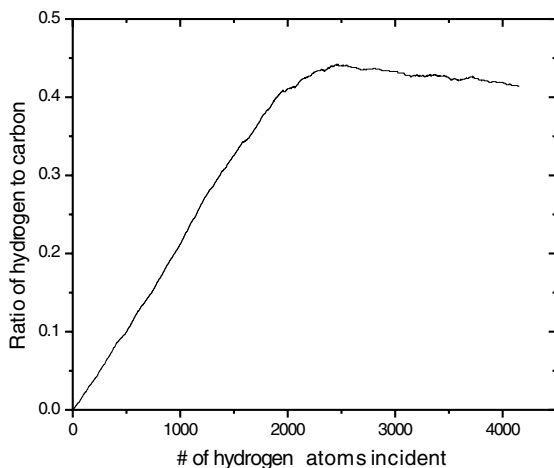


Fig. 1. Evolution of the H:C ratio of the originally pure graphite surface during 20 eV hydrogen bombardment.

Fig. 1. The resulting surface is a hydrogenated graphite surface with 0.42 H:C, near what is typically found in experiments. This surface was then used in all subsequent simulations to represent a C:H surface relevant to fusion devices. The surface is near a steady-state, as the H:C ratio is not completely constant in Fig. 1. Since the limiting factor in preparing these surfaces is CPU time, work on preparing this and other surfaces is an ongoing project.

2.2. Reflection calculations

The pre-prepared hydrogenated graphite surface described above was used as input to all of the following reflection calculations. Carbon at 45° and 60°, and some hydrocarbon molecules (CH, CH₂, CH₃, and CH₄) at 45° were incident on the surface at 300 K. Incident energies ranged from thermal to approximately tens of eV, coinciding with the upper end of the energy range where the potential is valid. Molecules were rotated randomly so that they struck the surface in a different 3D orientation each time. Close to 2000 separate flights were run for each incident species and energy to develop good statistics, giving reasonably small errors in the reflection coefficient of generally under 5%.

In order to run the necessary number of flights for each incident species/energy/angle combination, distributed computing was used to distribute the work among a collection of 10–20 PCs in the laboratory. The MD code benefits from multiprocessor-like speed-up by using idle CPU cycles that would otherwise be wasted.

3. Results

The reflection coefficients for carbon incident on the C:H surface at 45° and 60° are shown in Fig. 2. There tends to be a slightly higher probability of reflection in the case of the more glancing angle, as would be expected. When the surface was bombarded by hydrocarbon molecules, the reflection behavior became more complicated, as the molecules often break up into fragments. This can clearly be seen in Fig. 3, showing that for methane incident on the surface, reflection of any of seven different atoms or molecules may result. To summarize these results, the total carbon recycling can be calculated by summing the number of carbon atoms reflected in the form of all fragments, and dividing by the number incident. Fig. 4 shows such a calculation for all of the incident species investigated, i.e. C, CH, CH₂, CH₃, and CH₄.

Investigation of Fig. 4 reveals that the tendency of molecules to stick to the surface depends on the hydrogen content of the molecule. Methane, a saturated molecule, does not stick at thermal energies. At higher energies, the original CH₄ molecule can break

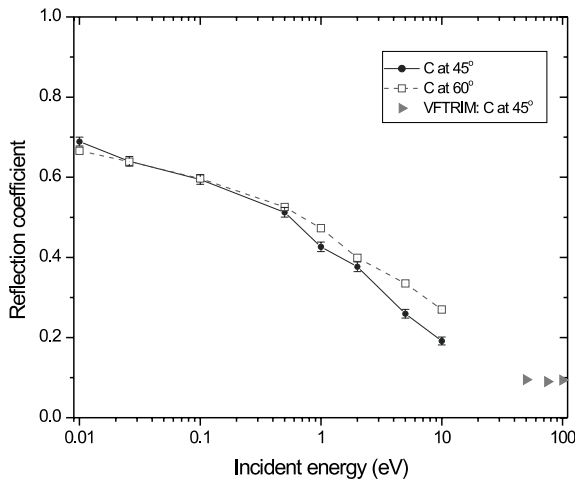


Fig. 2. Calculated reflection coefficient for carbon incident at 45° and 60° on a C:H surface. The error for the 60° case is not shown, but is comparable to that of the 45° case. Also shown for comparison is carbon reflection coefficient at 45° on a similar surface as calculated by VFTRIM-3D. The error in the VFTRIM-3D data is ± 0.003 .

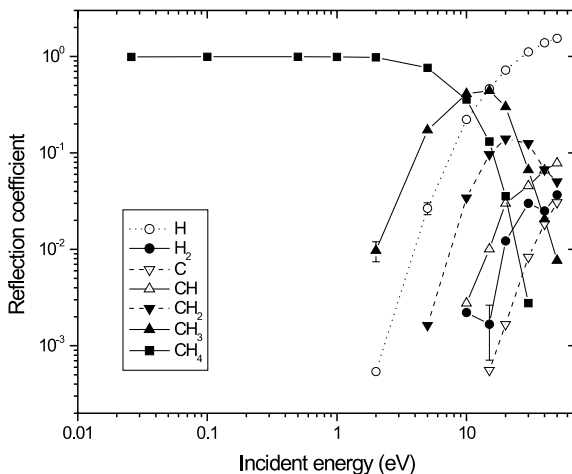


Fig. 3. Reflection of various species for CH_4 incident at 45° on a C:H surface.

up – allowing the fragments to stick to the surface more readily. As the hydrogen content was decreased in the radicals (from CH_3 to CH_2 to CH), the probability of sticking increased.

Also of importance for erosion/redeposition modeling is the energy and angle that particles are reflected with. For example, Fig. 5 shows that carbon atoms incident at 45° are reflected with an average energy near 32% of their initial energy. Also for carbon at both 45° and 60° (measured from normal), Fig. 6 shows that atoms tend to continue in the forward direction when reflected. This effect is more pronounced in the 60° (more

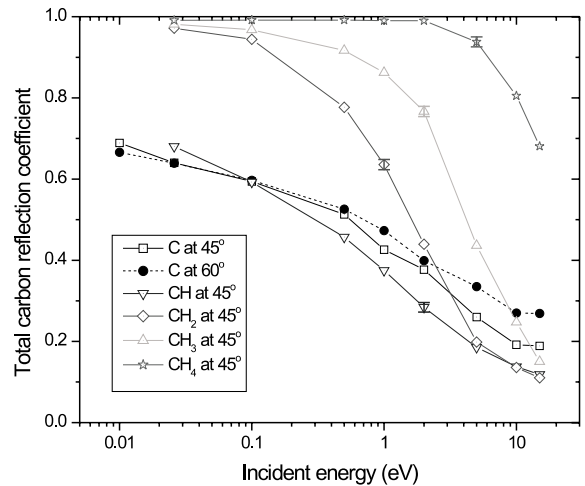


Fig. 4. Total carbon reflection coefficient for various species incident on a C:H surface at 45°.

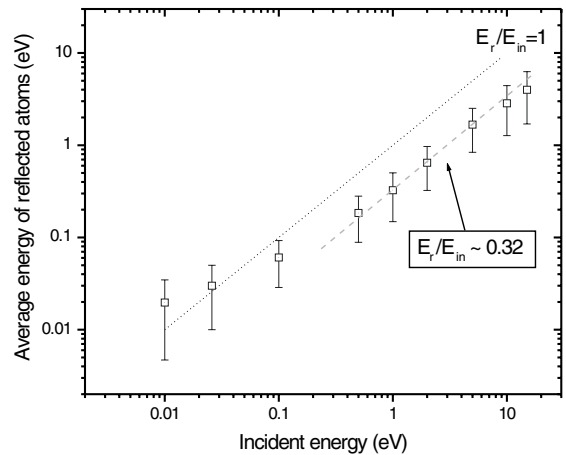


Fig. 5. Average energy of reflected particles for carbon incident at 45°, typically $\sim 32\%$ of incident energy. The error bars show the standard deviation in the reflected energy distribution.

glancing angle) case. The elevation angle distributions of reflected carbon atoms for both cases are shown in Fig. 7. Both peak near 45°, however in the 60° case a tendency to reflect specularly at 60° is evident. The standard deviation in the distributions are $\sim 15\text{--}20^\circ$ in the elevation angle and $\sim 70^\circ$ in the azimuthal direction.

Molecules seem to behave similarly, i.e. reflect with a similar fraction of their incident energy and at similar angles, although this is complicated by their tendency to break apart upon impact.

4. Discussion

An attempt has been made to draw a comparison between these results and that of the Monte Carlo code

VFTRIM-3D [8]. The surface in the VFTRIM-3D code was setup to approximate the surface used in the MD

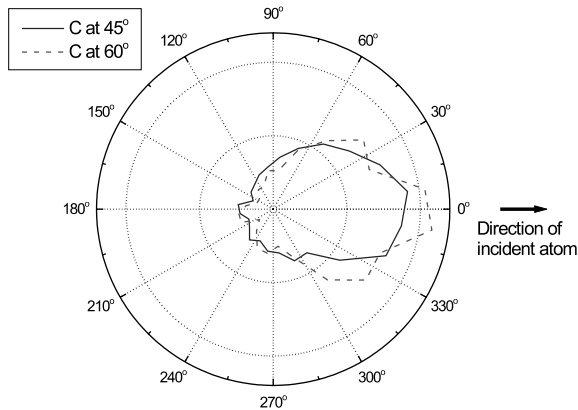


Fig. 6. Azimuthal angle distribution for reflected carbon atoms incident at 0.0259 eV, and at 45° and 60°, showing that particles generally continue in the forward direction when reflected. This effect is more pronounced in the 60° (more glancing angle) case.

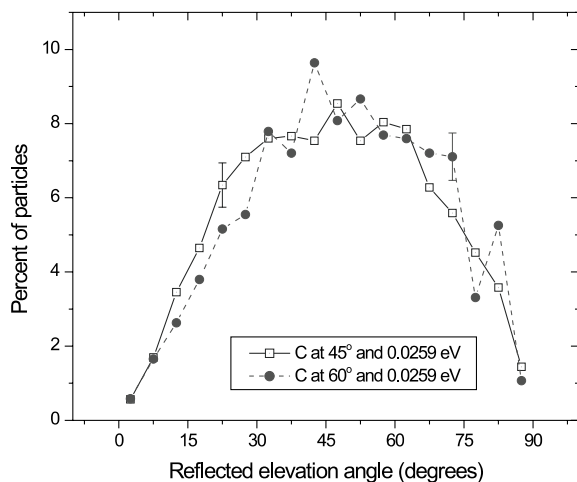


Fig. 7. Distribution of reflected elevation angles for carbon atoms incident at 0.0259 eV, and at 45° and 60°. Both distributions are peaked near 45°, but the 60° incident case shows a specular component around 60°.

calculations, i.e. it had the same H:C ratio, density, and surface binding energy. The calculated reflection coefficients at 45° show reasonable agreement as shown in Fig. 2, however a direct comparison is somewhat difficult. The main problem is that the two codes have different energy ranges in which they are valid. The Brenner potential used here is intended to describe the chemical bonding in carbon–hydrogen systems. However, its description of the repulsive, close interactions is too weak. Therefore, the MD modeling presented here is only valid up to the tens of eV energy range. VFTRIM-3D, on the other hand is based on the binary collision approximation, which is not valid at low energies where chemical bonding and many-body interactions become important.

A similar comparison has been made at the low energy end of the simulations. In this case, the modeling can be compared to the experimental data on hydrocarbon sticking or ‘surface loss probabilities’ summarized in Table 1. In the data, the surface loss probability represents the upper limit of the sticking coefficient and is defined as the sum of the probability of sticking and the probability of a reaction occurring at the surface that

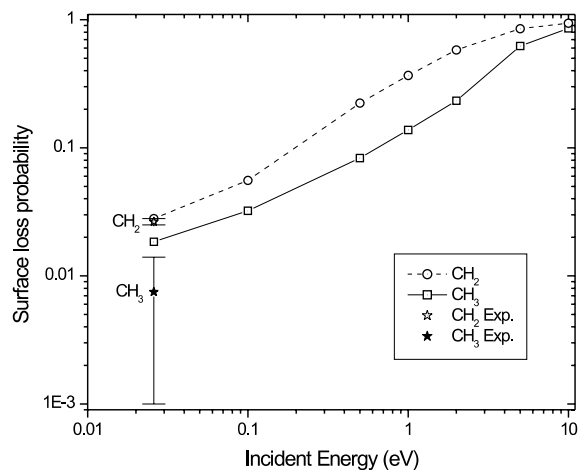


Fig. 8. Comparison of present modeling to experimental surface loss probabilities of CH₂ and CH₃. The error bars on experimental data represent the variation in the measurements.

Table 1

Summary of experimental data on sticking/surface loss probability of relevant hydrocarbons

Species	Surface loss probabilities	Sticking probabilities	Method	Reference
CH ₂	0.025–0.028		Decay in the afterglow	[9]
CH ₃	<10 ⁻³		Decay in the afterglow	[10]
	10 ⁻³ –0.014		Decay in the afterglow	[11]
	<0.014	0.006	Modeling of ITMS result measured with differentially pumped HIDEN MS	[12]
		10 ⁻⁴ –10 ⁻²	Radical beam experiments	[13]

results in a non-reactive volatile molecule. The comparison in Fig. 8 shows good agreement between the present simulations and previous experiments for CH₂ and CH₃ at thermal energy.

One of the most interesting results involving carbon PFCs is the large amount of tritium found in carbon deposits on the inner louver region in JET following a 2000 pulse (~10 000 s of operation) campaign using the Mk IIA divertor. This problem was analyzed in [14] using improved models for eroded carbon transport, including the reflection data for carbon and hydrocarbons presented here.

5. Conclusions

Reflection data for carbon and several hydrocarbon molecules (CH, CH₂, CH₃, and CH₄) has been calculated using a MD code. The reflection probabilities calculated compare reasonably well with those from VFTRIM-3D modeling at the upper end of the energy range, and with hydrocarbon sticking data at thermal energy. Key results, including reflection coefficients and reflected energy and angular distributions, can and have been included in erosion/redeposition codes to improve the capability of modeling chemically eroded carbon transport in fusion devices, such as in the problem of large amounts of tritium-containing carbon deposits in the JET Mk IIA divertor or in predictions of tritium retention/transport in ITER.

Future work will include determination of reflection data for the whole spectrum of hydrocarbons that come about due to chemical sputtering. Different conditions will be investigated, including different target surfaces. For example, graphite surfaces in tokamaks may actually consist of so called 'soft' redeposited carbon layers that are polymer-like, with higher hydrogen concentrations and lower densities. Also, the effect of different parameters needs to be studied, including incident angle and surface temperature. Finally, development of the

MolDyn code has progressed to the point that it can serve as a tool for other types of plasma–surface interaction analysis. An example of this is the simulation of liquid lithium surfaces in [15].

Acknowledgements

The authors would like to thank Jeffrey Brooks for motivating this work, Robert Averback for providing the MolDyn code used as a starting point, and Jean Paul Allain for his work with VFTRIM-3D. This work was supported by the United States Department of Energy under a subcontract from Argonne National Laboratory, no. DOE ANL 980332401.

References

- [1] B.V. Mech, A.A. Haasz, J.W. Davis, *J. Nucl. Mater.* 241–243 (1997) 1147.
- [2] J.N. Brooks, *Phys. Fluids B* 2 (1990) 1858.
- [3] K. Beardmore, MolDyn, Loughborough University, UK.
- [4] D.W. Brenner, *Phys. Rev. B* 42 (1990) 9458.
- [5] G.C. Abell, *Phys. Rev. B* 31 (1985) 6184.
- [6] J. Tersoff, *Phys. Rev. B* 37 (1988) 6991.
- [7] H.J.C. Berendsen, J.P.M. Postma, W.F. van Gunsteren, et al., *J. Chem. Phys.* 81 (1984) 3684.
- [8] D.N. Ruzic, *Nucl. Instrum. and Meth. B* 47 (1990) 118.
- [9] H. Toyoda, H. Kojima, H. Sugai, *Appl. Phys. Lett.* 54 (1989) 1507.
- [10] H. Kojima, H. Toyoda, H. Sugai, *Appl. Phys. Lett.* 55 (1989) 1292.
- [11] M. Shiratani, J. Jolly, H. Videlot, et al., *Jpn. J. Appl. Phys.* 36 (1997) 4752.
- [12] P. Kaenune, J. Perrin, J. Guillon, et al., *Plasma Sources Sci. Technol.* 4 (1995) 250.
- [13] A. von Keudell, T. Schwarz-Selinger, M. Meier, et al., *Appl. Phys. Lett.* 76 (2000) 676.
- [14] J.N. Brooks, A. Kirschner, D.G. Whyte, et al., these Proceedings. PII: S0022-3115(02)01405-8.
- [15] J.P. Allain, M.D. Coventry, D.N. Ruzic, these Proceedings. PII: S0022-3115(02)01371-5.